Scanning Near-Field Optical Microscopy and Scanning Thermal Microscopy

Jpn. J. Appl. Phys. Vol. 33 (1994) pp. 3785–3790
Part 1, No. 6B, June 1994

Scanning Near-Field Optical Microscopy and Scanning Thermal Microscopy

Russell J. PYLKKI, Patrick J. MOYER and Paul E. WEST
TopoMetrix Corp., 5403 Betsy Ross Drive, Santa Clara, California 95054-1162, USA

(Received January 25, 1994; accepted for publication April 16, 1994)

The development of the scanning tunneling microscopy has led to the development of related techniques which include the scanning near-field microscopy (SNOM) and the scanning thermal microscopy (SThM). These techniques provide sample information in addition to the simultaneously obtained topography. With SNOM normal optical microscopy contrast mechanisms (adsorbance, fluorescence, polarization, etc.) can be used. The principles and design of a SNOM are presented. Subwavelength resolution (better than $\lambda/20$) is demonstrated. In SThM, the contrast is provided by temperature and thermal conductivity. The design of a resistive thermal probe is described. Several operating modes are described and image contrast due to thermal conductivity is demonstrated.

KEYWORDS: scanning near-field optical microscopy, scanning thermal microscopy, scanning tunneling microscopy and atomic force microscopy

1. Introduction

Since the development of the scanning tunneling microscope (STM), many "daughter" scanning probe microscopes (SPM) have been introduced, including the atomic force microscope (AFM), the magnetic force microscope (MFM), the electrochemical AFM and STM, the scanning thermal microscope (SThM) and the scanning near-field optical microscope (SNOM), to name just a few.[1] These techniques are very similar to the STM in design, but are based on a variety of tip-sample interactions, and hence, differing contrast mechanisms. SNOM brings to the SPM family an optical probe that can yield complementary information to the other techniques that can only be obtained by optical means. For example, contrast mechanisms available only to optical probes such as absorption, polarization, and reflectance, as well as spectroscopic methods, such as luminescence,[2] emissions, fluorescence, and Raman scattering[3] are some of the major advantages of being able to extend the capabilities of SPM for a more complete characterization on the nanometer scale of investigation. In SThM, the tip-sample interaction is based on heat flux, therefore differences in temperature and thermal conductivity provide the contrast mechanism. It is difficult, if not impossible, for traditional techniques to directly measure the thermal properties of microscopic features such as whiskers, grains and grain boundaries. The capability to measure these properties on a microscopic scale is important in the development of materials themselves and should provide better interpretation and modeling of their bulk properties. The capability to map temperatures with submicron resolution is of obvious interest to the microelectronics industry. A resistive thermal probe is described which has the flexibility to measure both temperature and thermal conductivity.

2. Scanning Near-Field Optical Microscope

Scanning near-field optical microscopy (SNOM)[4,5] is a relatively new method of optical microscopy that allows for imaging with resolution not previously afforded by optical techniques. SNOM overcomes the conventional Abbe barrier, or diffraction limit, of resolution to allow optical characterization techniques to keep up with the technological trend of miniaturization. Optical microscopy is the oldest and remains the most widely used form of microscopy, despite the onslaught of ultra-high spatial resolution electron, ion, and scanning probe microscopes. The contrast mechanisms and high resolution of the latter techniques render them invaluable for a number of high technology applications. However, optical microscopy provides a number of inherent advantages that cannot otherwise be achieved. First, the contrast mechanisms are those utilized by the human eye, making image interpretation simpler. In addition, the probing techniques are typically noninvasive to the sample, and thus, samples studied in investigative research areas such as biology, medicine, and genetics can often be investigated in their native environment. This prevents indeterminable image artifacts that may arise during sample preparation or the behavior of the sample in an 'unfriendly', or unnatural environment. Finally, and perhaps most importantly, through a number of spectroscopic techniques, chemical species can be identified by investigating fluorescence and bonding characteristics of the sample.

The major disadvantage of conventional optical microscopy is the resolution limit imposed by the effects of far-field diffraction. This limit, which theoretically is about 200 nm for green light (λ=500 nm), is more on the order of 500 nm in practice. Thus, in a scientific world where semiconductor line widths are approaching a few tenths of a micron, and cell and molecular biology are currently characterizing routinely on a tenth micron scale, optical microscopy appears to have limited use.

By providing an optical characterization technique with most of the same contrast mechanisms available to conventional optical microscopy, SNOM improves spatial resolution by more than an order of magnitude. In 1928, E. H. Synge suggested the possibility of overcoming the conventional far-field diffraction barrier by fabricating an optical aperture much smaller than the wavelength of light and positioning the aperture from the sample at a distance that is much smaller than the wavelength of light.[6] By using the aperture as a light source, image resolution would be limited to the size of

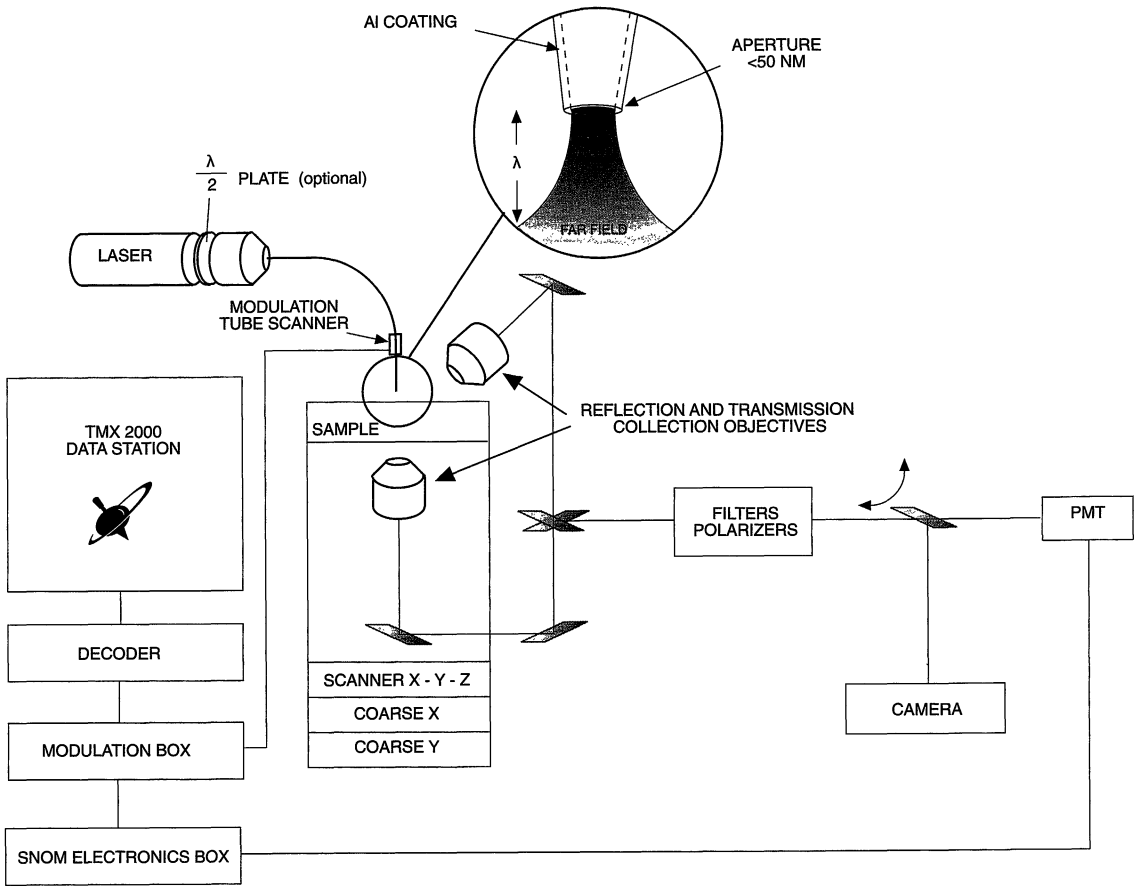

Fig. 1. Schematic diagram of the SNOM instrument.

the aperture, and not by the wavelength of light. This experiment was not feasible at optical frequencies in the 1920's due to the difficulty in controlling and manipulating such a structure with the precision necessary. In 1972, near-field imaging resolution of $\lambda/60$ (0.5 mm) was demonstrated at microwave frequencies, where positioning requirements are relatively simple.[7] Finally, in 1982 the technology necessary for experimentally realizing near-field optical microscopy was brought to bear with the development of the STM by Binnig and Rohrer.[8] Pohl *et al.*[4] showed $\lambda/20$ SNOM imaging resolution in 1984.

A schematic diagram for the SNOM used to obtain the data presented here is shown in Fig. 1. The microscope is designed to operate in either the reflection mode or the transmission mode. In the transmission mode, transparent and weakly absorbing materials can be studied, such as biological specimens and semiconductor thin films. The transmission mode typically provides a higher signal throughput due to the forward scattering detection direction and the lack of an obstruction from the tip. In the reflection mode, a wider range of samples can be studied. Although the detected signal is slightly lower than in the transmission mode, the information detected is mostly from the surface and image resolution is excellent. Another advantage of operating in the reflection mode is for biological fluorescence. The fluorescence is essentially uniformly scattered, while the excitation wavelength is predominantly forward scattered. Thus, in the reflection mode, the detected background signal from the incident wavelength is lower than in the forward scattered transmission mode.

The light emanating from the aperture is rapidly diverging to the extent that a 15 nm variation in tip-sample separation results in a significant change in the image resolution. Thus, it is crucial that a constant tip-sample separation be maintained. This is done using shear force detection and a feedback loop.[9] The tip is oscillated parallel to the sample surface at its fundamental resonant frequency (~30–130 kHz) with an amplitude of about 5-10 nm. As the tip approaches the surface, interaction with the contamination layer (i.e., water vapor, etc.) on the tip and sample damping the amplitude and shifting the phase of the oscillation. By monitoring the phase shift of the interaction and maintaining a slight change in this phase, the tip can follow the topography of the sample. The result is that a topography map and an optical SNOM image can simultaneously and independently be acquired. This type of force feedback can also be employed in liquid. The damping of the free vibration resonance upon contact with the liquid decreases the Q-factor of the probe, and hence, the sensitivity of the force measurement decreases by approximately a factor of three. The force feedback signal still allows for sufficient feedback to

yield necessary tip-sample distance control for high resolution SNOM imaging.

As is the case with any scanned probe microscopy, it is important to understand the physics of the tip-sample interaction for SNOM experiments. With an optical fiber serving to illuminate the localized region of the sample, we can understand the nature of the SNOM near-field interaction based on fiber-optic waveguide theory.[10] This helps to understand how the light is coupled out of the aperture and into the near-field. The mode describes the electric field strength as a function of radial distance from the center of the core. Briefly, the mode structure of the fiber provides two major advantages. First, the ability of the fiber to propagate light with very low losses allows a significant amount of power to be coupled to the aperture region. Although for subwavelength sized apertures, the coupling efficiency through the aperture and into the near-field is quite low (as low as 10^{-6}), most of the light is lost at the tip and not through propagation to the tip region. Secondly, the mode structure of the fiber provides one with a fundamental understanding of how the sample is being illuminated. Investigating the spatial distribution of the intensity of the light as a function of lateral dimensions and waveguide parameters helps to understand the imaging mechanism and the capabilities and potential limits of SNOM.[10]

As an example of the resolution capabilities of the instrument and application to a biological sample, Fig. 2 shows a SNOM image of tobacco mosaic virus (TMV) particles. The TMV particles were covalently attached to amino-silanated mica using gluteraldehyde (0.04%–0.08%). After several minutes the gluteraldehyde was removed by rinsing in distilled water, excess water was removed and the sample was imaged immediately. The image, obtained in the transmission mode, was obtained using an Argon ion laser of wavelength $\lambda=488$ nm as the light source. The features are clearly imaged with higher localization than can be provided with a conventional far-field microscope. Additionally, as this image is $1.4\times1.4\,\mu m^2$, individual TMV particles are resolvable with separations of less than 30 nm. Thus, this data clearly shows the resolution capabilities of the SNOM technique.

Figure 3 illustrates the simultaneous force and SNOM data acquisition capabilities of the instrument. This data is taken from retinal eye tissue of a rat. The data is also taken in the transmission mode so some of the variation in the SNOM image corresponds to changes in tissue, which can be seen in the topography image. This sample has been microtomed and fixed in resin on a glass microscope slide substrate.

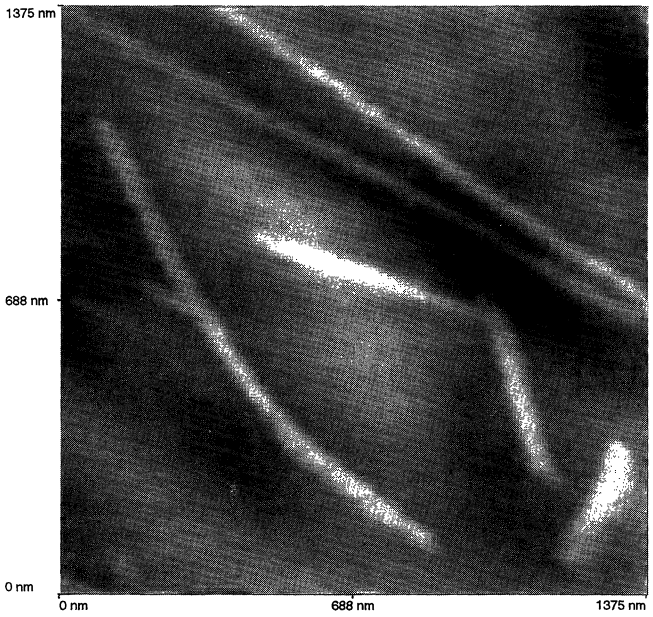

Fig. 2. Transmission SNOM image of tobacco mosaic virus macromolecules.

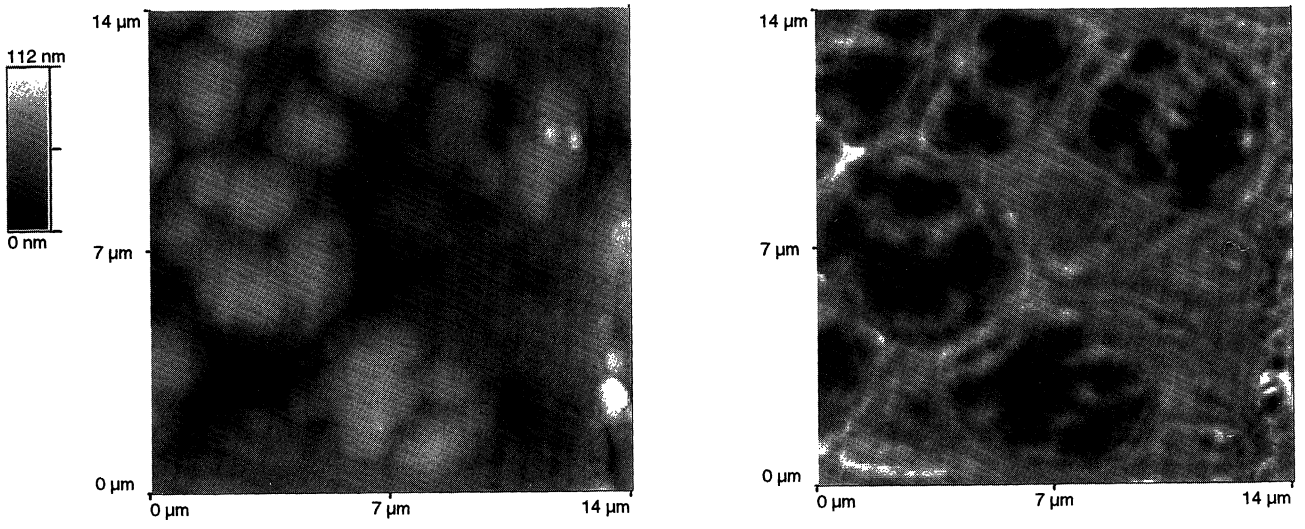

Fig. 3. Simultaneous topographic and transmission SNOM images of retina tissue taken from a rat's eye.

3. Scanning Thermal Microscopy

The first use of a thermal probe with a Scanning Probe Microscope (SPM) was reported in 1986.[11] At that time, the Atomic Force Microscope (AFM) had not yet been developed and Williams and Wickramasinghe overcame the inability of the scanning tunneling microscope (STM) to image non-conductive surfaces. In their initial application, the thermal probe was fashioned by forming a thermocouple on the apex of a tungsten STM tip. The probe was heated and brought to near contact of the surface. When the thermal diffusion layer surrounding the heated probe overlaps the substrate, heat is transferred to the substrate, cooling the tip and signaling the presence of the surface. Since the thermal conductivity of solids is generally much greater than that of air, the probe tends to sense the proximity of the solid only, independent of its thermal properties. The probe is scanned parallel to the sample surface while moving the tip normal to the surface as necessary in order to maintain the tip at a constant temperature allowing the surface profile to be determined.

Advancements in the technique include forming the thermocouple junction between a metal probe and a conductive substrate[12] to measure surface temperatures. The same technique was later used with a heated probe to detect changes in subsurface thermal conductivity.[13] More recently, AFM cantilever has been fashioned which form a thermocouple junction at the scanning tip.[14] This development allows temperatures of non-conductive surfaces to be studied.

In contrast to the thermocouple probes described above, we have integrated a resistive thermal probe with an AFM cantilever.[15] The temperature of the probe is monitored by measuring its resistance. The probe can be used in two general modes. In the "passive" mode the probes temperature is monitored as it is scanned across the surface. The constant current passing through the probe to measure its resistance is small such that negligible self-heating occurs. In this mode the probe is primarily sensitive to the temperature differences between the probe and the sample rather than differences in samples thermal conductivity.[14] In the "active" mode, larger currents are passed through the probe to induce resistive heating. In this mode, the heat flow between the probe and sample will be influenced by the thermal conductivity of the sample in addition to the temperature difference. The "active" probe may be operated in either a constant current or a constant temperature mode. As the name implies, in the constant current mode, a constant current is passes through the probe and changes in heat flux between the probe and sample are detected as changes in the probe resistance. In contrast, in the constant temperature mode, the voltage applied to the probe is changed as necessary to maintain a constant resistance (constant temperature). The constant temperature mode has the advantage of an inherently fast probe response time. Since the probe is maintained at a constant temperature, the system response is not limited by the need to establish a new thermal equilibrium in the probe that occurs when is used in either the "passive" or "active" constant current modes. The result is that a constant temperature probe has a response time on the order of 10 μs versus 1 ms for the 'passive' probe.

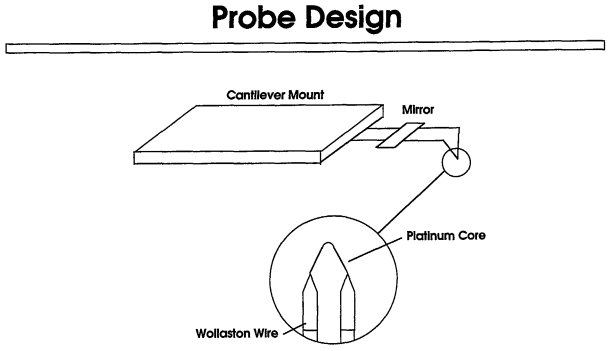

Fig. 4. Simplified schematic diagram of the resistive thermal probe.

The thermal probes are fashioned from Wollaston process wire. This material typically consists of a platinum core (*ca.* 5 mm diameter) surrounded by a thick silver sheath (*ca.* 75 mm). The surrounding silver creates a wire thick enough to be easily manipulated. A loop of the Walloston process wire is formed (Fig. 4) and attached to the cantilever carrier forming the arms of the cantilever (*ca.* 5 mm long). Once the wire is properly oriented, the silver at the end of the loop is etched, uncovering a small length of the platinum (*ca.* 200 μm). When a current is passed through the cantilever loop, heating occurs primarily in this exposed platinum filament because it has the only significant resistance of the probe. A small piece of aluminum coated tape is cemented across the arms of the cantilever to provide the mirror for optical beam detection of the cantilever movement.

Thermal control of the probe is achieved by making it part of a bridge circuit. The probe forms the only element in the circuit whose resistance is sensitive to the voltage across the circuit. In the constant current modes, changes in the probe temperature are observed by monitoring the bridge balance. In the constant temperature mode, a feed back loop is employed which adjusts the voltage applied to the bridge circuit to keep it balanced. Heat flux from the probe is observed by monitoring the voltage applied to the circuit.

In Fig. 5, the thermal probe is scanned across a test grid of silicon oxide (ca. 200 nm thick) on a silicon substrate. The silicon has a higher thermal conductivity (148 W/mK) than the oxide overlayer (1.4 W/mK). The probe was held at 20°C above room temperature, scanned at 200 μm/s and operated in the constant temperature mode. The thermal image was obtained by recording the bridge voltage. The topography is shown in Fig. 5(a), while the simultaneously obtained thermal image is shown in Fig. 5(b). Due to the differences in thermal conductivity, more heat flows from the probe

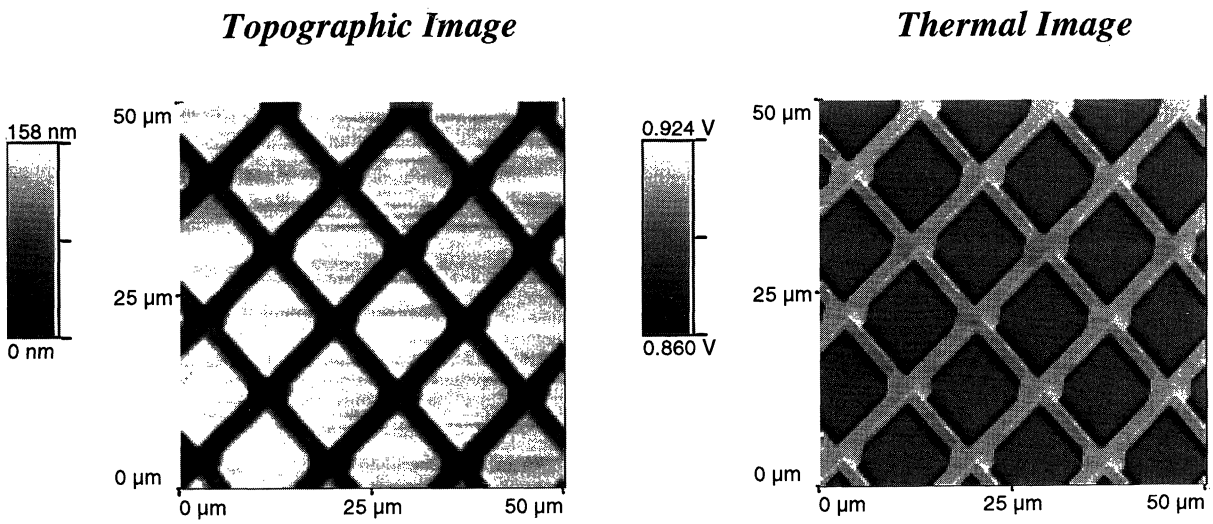

Fig. 5. Simultaneous topographic and thermal image of a test pattern of silicon oxide (10 μm × 10 μm) on silicon. Thermal image contrast caused by differences in thermal conductivity.

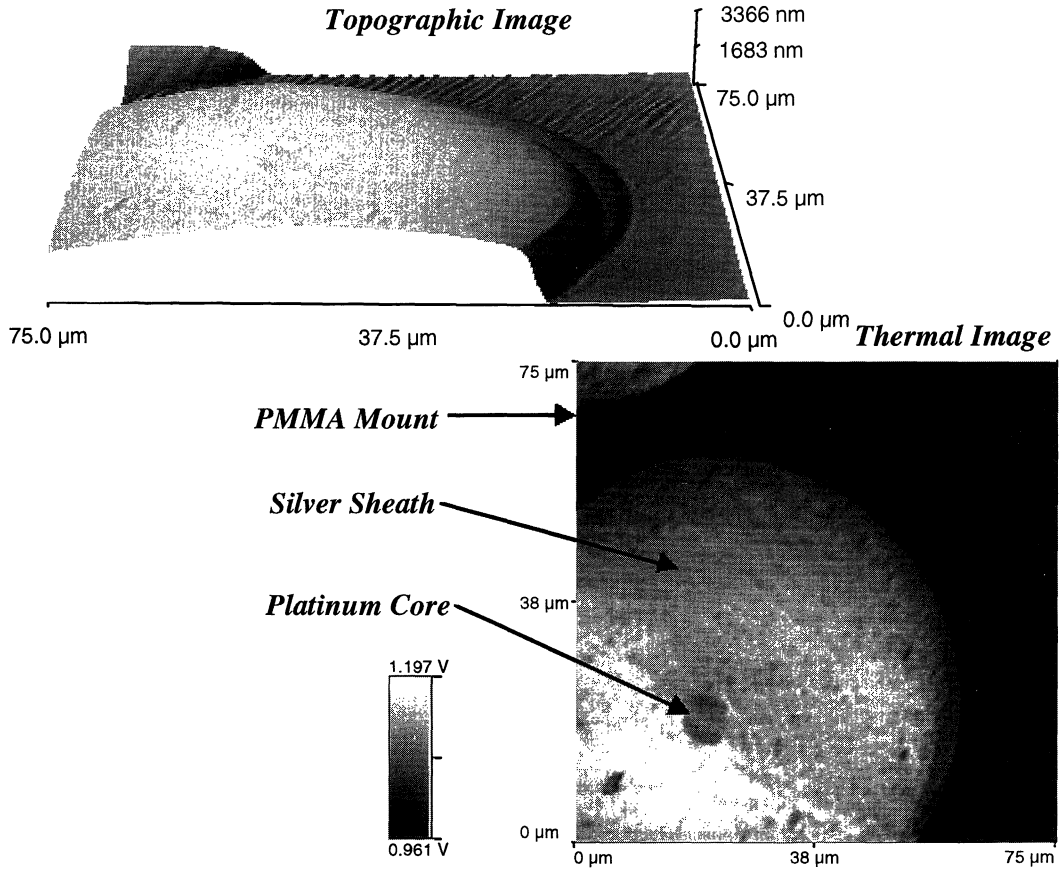

Fig. 6. Simultaneous topographic and thermal image of Wollaston process wire (cross-section) mounted in poly-(methylmethacrylate). Thermal image contrast caused by differences in thermal conductivity.

to the sample when it is in contact with the silicon than the silicon oxide so these areas appear brighter in the thermal image. The structure on the thermal image clearly corresponds with the feature of the topographic image. Similar images were abtained when scanning at 20 and 1000 μm/s.

In Fig. 6, a cross-section of Wollaston process wire was imaged. The wire was mounted in poly-(methlymethacrylate) (PMMA) and the final polish used a 0.05 μm chemically-assisted media (Masterpolish II, Beuhler). The topography in Fig. 6(a) clearly shows the wire protruding above the PMMA mount.

This is a polishing artifact caused by the disparity in hardness between the materials. In the thermal image (Fig. 6(b)) the increased thermal conductivity of the silver (417 W/m-K) versus the PMMA (0.2 W/m-K) is clearly shown. In addition, the reduced thermal conductivity of the platinum core (71 W/m-K) versus the surrounding silver can also be seen.

Current work on the thermal probes is directed to increasing the lateral resolution (currently about 0.5 μm) and to calibration based on thermal conductivity. In addition, the use of the probe to measure sample temperatures will be demonstrated in the near future.

4. Conclusions

In conclusion, with the technological demand for decreasing dimensional analysis we have shown the potential value of an instrument that can maintain optical characterization capabilities with the improvement in spatial resolution (better than $\lambda/20$) that conventional far-field microscopy can not attain. In addition, a resistive thermal probe has been developed. The capability of the probe to provide contrast based on the thermal conductivity of the sample has been demonstrated.

1) R. Pool: Science **247** (1990) 634.
2) M. A. Paesler, P. J. Moyer, C. L. Jahncke, C. E. Johnson, R. C. Reddick, R. J. Warmack and T. L. Ferrell: Phys. Rev. B **42** (1990) 6750.
3) P. J. Moyer: PhD Thesis, North Carolina State University (1993).
4) D. W. Pohl, W. Denk and M. Lanz: Appl. Phys. Lett. **44** (1984) 651.
5) for a good review, see Eric Betzig and Jay Trautman: Science **257** (1992) 189.
6) E. H. Synge: Phil. Mag. **6** (1928) 356.
7) E. A. Ash and G. Nicholls: Nature **237** (1972) 510.
8) G. Binnig, H. Rohrer, Ch. Gerber and E. Weibel: Phys. Rev. Lett. **49** (1982) 57.
9) E. Betzig, P. L. Finn and J. S. Weiner: Appl. Phys. Lett. **60** (1992) 2484.
10) E. L. Buckland, P. J. Moyer and M. A. Paesler: J. Appl. Phys. **73** (1993) 1018.
11) C. C. Williams and H. K. Wickramasinghe: Appl. Phys. Lett. **49** (1986) 1387.
12) J. M. Weaver, L. M. Walpita and H. K. Wickramasinghe: Nature **342** (1989) 783.
13) M. Nonnenmacher and H. K. Wickramasinghe: Appl. Phys. Lett. **61** (1992) 168.
14) A. Majumdar, J. P. Carrejo and J. Lai: Appl. Phys. Lett. **62** (1993) 2501.
15) R. B. Dinwiddie, R. J. Pylkki and P. E. West: to be published in *Thermal Conductivity 22*, ed. T. W. Tong (Technomic Publishing Co., Lancaster, PA, 1994).